INTER COLLEGAS, VOL. 4, No.3 (2017)
ISSN 2409-9988

SURGERY

Rzechonek A [1]., Blasiak P [1]., Muszynska-Bernhard B[2]., Adamiak J[2]., Grzegrzółka J.[3]., Majchrzak M[1]., Budzynski W [4]., Le Pivert P[5].

THE BI-DIRECTIONAL MIGRATION OF A DYE TRACER INJECTED AT THE EDGE OF PRIMARY OR SECONDARY LUNG TUMORS DURING SURGERY. INITIAL STUDY ON 33 PATIENTS AND CLINICAL IMPLICATIONS

1 - Department of Thoracic Surgery, Wroclaw Medical University
2 - Department of Pathology, Lower Silesian Centre of Lung Diseases,
3 - Department of Histology and Embryology, Wroclaw Medical University
4 - Biotech
5 - Interventional Drug Delivery Systems and Strategies (ID2S2)

Abstract: Purpose. To assess the loco-regional distribution pattern of a blue dye tracer, as a surrogate for a chemotherapeutic agent, injected in the invasion edge of resectable lung tumor; to evaluate the technique efficacy at staining the lung-tumor interface and the metastatic pathways. Methods. Between November 2014 and September 2015, we enrolled 33 patients (17 women, 16 men; 52-87 years old) presenting with 31 primary lung carcinomas and 2 metastases. We injected in vivo (n=17) or ex vivo (n=16) the innermost side of the tumor invasion edge with 1.3ml methylene blue dye. We performed the injection alone (n=12) or combined with a focal freezing (n=21). We assessed the stain distribution into the invasion-edge, the tumor, the lung or the node(s) at gross and microscopic examination. Results. At gross examination, we observed a quick, intense staining of the invasion edge, and a concomitant staining of the tumor and the lung. The staining pattern was heterogeneous in the tumor, homogeneous in the invasion edge and the lung irrespective of the focal freezing, tumor type, size, or blood perfusion status. The microscopic examination evidenced the staining of the matrix, vessel lumens, and tumor cells, except for lymph nodes. Conclusions. The inner side of the invasion edge looks a suitable location for directly injecting and distributing the methylene blue tracer within the interstitium and related draining pathways during the resection of primary or secondary lung tumor. Fresh resection specimens are convenient to evaluate new edge-targeting injections techniques for the diagnostic or therapeutic management of cell dissemination during surgery.

KeyWords: freezing-assisted injection, lung tumor, methylene blue, surgery, tumor edge injection.

INTRODUCTION

The resection of the primary tumor and loco-regional lymph nodes is the best curative option for stage I to IIIA NSCLC, but the rate of loco-regional and local plus distant recurrences after curative surgery, respectively 17% to 27% and 39% is high [1]. Adjuvant systemic chemotherapy (ACT) has demonstrated modest survival benefit largely confined to patients with stage II disease [2].

Corresponding Author:
Adam Rzechonek MD, Department of Thoracic Surgery, Wroclaw Medical University.
E-mail: adam.rzechonek@gmail.com

Many studies suggest that surgery has a pro-metastatic effect potential, likely affecting the disease free survival (DFS) and the overall survival (OS) rates [3, 4, 5, 6]. The search for new multimodal anti-metastatic therapeutic strategies has lead oncologists to consider the initiation of adjuvant chemotherapy during the perioperative period, regarded as a "window of opportunity [3], and/or the loco-regional administration of active agent (s) [7]. Many advocate a more systematic use of the combination of adjuvant chemotherapy and resection for early lung cancer [8].

The metastatic dissemination, arising from a growing tumor, a surgical resection [5, 6] or a biopsy [9] involves cells shedding within the tumor interstitium and the aerial, hematogenous and/or lymphatic drainage pathways, [10,

11]. Thus, the tumor interstitium has increasingly become a target for various diagnosis and therapeutic agents [12]. The peritumoral (PT) and/or intratumoral (IT) injection of chemotherapeutic (CT) agents has emerged as a useful and efficacious method in controlling lung tumors [13, 14,]. The advantages of local over systemic chemotherapy [CT] are an elevated local drug concentration, little or no side effects, and the modulation of local plus distant antitumor immunity [15].

Whether the tumor approach is surgical, endoscopic or per-cutaneous, the gross tumor edge is the usual landmark for assessing the location of the injection needle (s), since it is a marker of the procedure realization and efficacy evaluation [16]. However, the spatial positioning of the needle is based on a rough estimate of the tumor edge, as exemplified with the high variability of results currently observed for lung cancer lymphatic mapping [17, 18]. Chemoablation, a therapeutic method that injects cytotoxics directly in multiple IT and PT sites shows undeniable local cell kill efficacy [14, 19]. Still the procedure lacks a precise spatial reference for the peritumoral needle insertion and therefore remains very operator-dependent. In this translational study, we propose to use a readily locatable region of the tumor edge as a spatial reference for the injection (s); a tumor region that interfaces with the adjacent lung parenchyma and possesses similar interstitial fluid transport characteristics [20].

We describe here the direct injection of a fixed dose of methylene blue dye (MB) in the innermost side of the tumor invasion edge (IE). MB is a small, weakly basic drug, a known localization-tracer for a lung tumor [21], a photosensitizer [22], and a lymphatic tracer [23]. This mono-institutional study includes 33 human patients presenting with resectable stage I-IIIA primary (n=31) or metastatic tumors (n=2). The primary objective was to investigate the MB migration rate, direction and pattern within the tumor and the lung draining pathways. A secondary goal was to assess the seamless integration of the procedure within the workflow of conventional surgery. We evaluated various injection strategies, whether injection was the sole modality or a combination with a nearby focal tumor freezing, and whether the procedure took place during or after the surgical resection. Therefore, we could compare the tracer migration in perfused, in vivo, and non-perfused, ex vivo, lung-tumor samples. The simultaneous focal freezing-and-injection aimed at evaluating whether the combined procedure would affect the dye migration pattern compared to the injection alone, as previously demonstrated in pre-clinical studies [24, 25].

2 PURPOSES, SUBJECTS and METHODS:

2.1 Purposes. Our primary goal was to develop a reliable injection technique of the inner side of the invasion edge of resectable lung tumors. We investigated at gross and microscopic examination the migration rate, direction and pattern of methylene blue (MB) within the tumor and the lung; we compared the staining results whether the injection was the sole modality or was associated with a nearby focal tumor freezing, and whether the procedure took place during or after the surgical resection. . Another goal was to assess the seamless integration of the procedure within the workflow of conventional surgery. The ultimate objective of our research is to use the knowledge gained from this study for the development of intraoperative, antimetastatic local drug delivery techniques during the surgery of lung tumors.

2.2 Subjects & Methods

This study was approved by the Ethics Committee of the Department of Thoracic Surgery, Wroclaw Medical University, Poland. Between November 2014 and September 2015, 33 operable patients had their tumor resected at thoracotomy (Table 1). The patients were chemotherapy naive. They provided their informed consent before the procedure. The clinical suspicion of malignancy was confirmed with preoperative biopsy (n=6), intraoperative incisional (n=20) or excisional biopsy (n=3)-, or core needle biopsy (n=4). The pathology was adenocarcinoma (ADC, n=16), squamous cell carcinoma (SCC, n=7), Large cell carcinoma (n=5), carcinoid (n=1), carcinosarcoma (n=1), small cell carcinoma (n=1), non-pulmonary metastasis

(n=2). Twenty-two of 33 patients presented with IA to IIB stage disease: IA (n=5), IB (n=7), IIA (n=5), IIB (n=5), or with IIIA stage disease (n=6).

Table 1.

Patients, tumors and disease stage

Patients, (33)	
mean age (range), years	*64 (52-87)*
Sex, Male, Female, (n)	*M (16), F (17)*
Histology	
ADC	*16*
SCC	*7*
Large Cell Ca	*5*
Carcinoid	*1*
carcinosarcoma	*1*
Small cell Ca	*1*
Meta (not lung)	*2*
Tumor Stage	
IA	*5*
IB	*7*
IIA	*5*
IIB	*5*
IIIA	*6*
IIIB	*2*
IV	*3*
Surgery	
Lobectomy	*25*
Segmentectomy	*2*
Wedge Resection	*4*
Pneumonectomy	*2*

UICC-Union for International Cancer Control;
ADC-Adenocarcinoma; SCC-Squamous Cell Carcinoma.

Surgery: Table 1 shows the surgical procedures. Except for the two metastasectomy, we performed a mediastinal lymph node dissection (MLD) in 29 patients and a mediastinal lymph node sampling at the hilar and mediastinal level in two. Following the biopsy, and ten minutes after the completion of the injection, lymphovascular dissection and resection procedure were conducted regardless of the staining results. Care of not disrupting the tumor lymphovascular draining pathways during the allotted migration time of the tracer off the injection side was taken. In most but not all patients, the pulmonary artery was ligated before the pulmonary vein. On average, it took 90 minutes from the end of the injection to the resection of the lung-tumor specimen. The total duration of the surgery was 141 minutes (ranging from 90 to 198 min). After the specimen resection and before the closure of the wound, the thoracic cavity was flushed with one liter of saline solution at room temperature.

Injection needle and cryoprobe: The prerequisites for the study were the selection of readily available user-friendly, low-cost instrumentation and drug tracer. For the injection, we used a commercial a 23 G, 50mm needle (BD, http://www.bd.com/pl/) and a self-made depth stop that makes the needle easier to manipulate and keep steady at a known depth, 15mm to 20mm, within the tumor edge, as seen in Figure 1. The needle was connected to a small bore extension line and a 3ml plastic syringe; the fluid line and needle were debubbled and primed before needle insertion; for the tumor edge freezing, a separate cryoprobe (Cp) with a cooling tip-3mm wide, 25mm long, was connected to a nitrous oxide powered console (CRYO-S-II electric, Metrum-CryoFlex, Warsaw, Poland). The cryosystem full functionality was checked prior to any clinical use. We had previously conducted in vitro simulations of the simultaneous freeze-and- injection, i.e. a freezing-assisted injection procedure to determine the temporospatial parameters of the fluid delivery illustrated at Figure 3. We determined that 3 minutes of continuous cooling make an average 3ml ice zone (IZ) in a hydrogel medium; the IZ is impervious to a solution of MB 1%; a 1.5ml volume of MB spreads over about 40% of the ice margin (Le Pivert, data not shown). We assessed in ex vivo freshly resected and deflated lung tumor samples the formation of a similar IZ shape and volume with the same cryoprobe and freeze duration (data not shown).

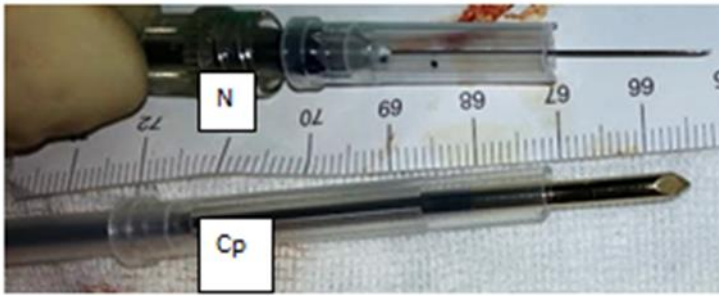

Fig. 1. (Left) Self-made needle (N) depth-stop for adjusting the insertion depth, ≤20mm. The cryoprobe (Cp) is inserted about 10mm apart from the needle. (Right) During surgery, the 23 G needle is seen located in the palpable edge of a peripheral lung tumor.

Methylene blue dye: Methylene blue (MB, American Regent, NY, USA) is a small (MW 319), nanosized molecule (5nm) that has a known safety, and tracing ability in lung tumor [26] and lymphatics [17, 26]. Our method delivers manually and continuously a fixed dose, 1.3 ml of undiluted 1% MB into the tumor invasion edge (IE) over a two minutes period. The dye dosing was calculated as the lowest amount susceptible to migrate within the IE interstitial fluids, the tumor and/or the lung parenchyma as demonstrated or inferred from previous studies [18, 27]. The MB is a weakly basic molecule that resembles some cytotoxics and tends to aggregate in acidic environment, a characteristic of the invasion edge fluids.

Injection procedure: We modelled the fluid space of the tumor invasion edge (Figure 2) as a torus having a mean thickness of 10mm (range: 7mm to 13mm). The torus center line is the tumor gross edge that comprises two fluid compartments: one stretches in the tumor inner side of the gross edge, 1mm [27] to 5mm thick; the other pervades the peritumoral and lung side of the gross edge, 6mm to 8mm thick [28]. It is the region of NSCL cancer microscopic extension. Based on literature [29, 30, 31], a common fluid space for both compartments, each having similar fluid pressure, hydraulic conductivity, and flow velocity was assumed. On a deflated lung, one inserts the needle, equipped with the depth stop, in the innermost side of the visible and/or palpable tumor edge, i.e. 1mm to 5mm inside the margin and 15mm to 20mm deep. We inject the tumor side that faces the interlobar fissure or hilum, a location estimated best for a rapid transport of the tracer in this direction, as shown in Figure 2.

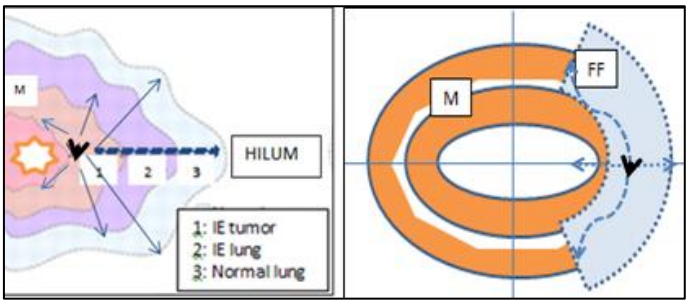

Fig. 2. (Left) Schematic representation of the invasion edge (IE) fluid compartments and injection strategy. (Left) Regions 1 and 2 are the inner and outer interstitial compartments of the gross tumor edge (M) that artificially distinguishes them. The needle (arrowhead) injects the tracer in the innermost side of region 1, and in the tumor quadrant facing the hilum. For the freezing -assisted injection procedure, we insert the cryoprobe (star) between the tumor center and the needle. The frozen tumor tissue surrounding the probe tip acts as an impervious mass to the penetration of the co-injected tracer [24, 25]. (Right) Our model assumes a similar fluid flow (FF) in the interstitial fluid compartments of the edge (M, white thick line), along with a similar tracer distribution rate, and pattern. The tracer migrates through the interstitial fluid pathways and the vascular drainage (thin dotted arrows and drawing area) towards the normal lung -3- and the hilum. The injection pressure drives a convergent fluid flow towards the tumor and a divergent flow towards the lung.

Freezing-assisted injection procedure: Our focal freezing-assisted injection procedure (FAI) derives from prior pre-clinical [24, 25] studies that demonstrated the transient imperviousness of the tissue undergoing freezing, i.e. the ice zone (IZ), to a locally co-injected tracer solution; we hypothesized that the IZ "barrier" would facilitate the channeling of the tracer in the low fluid-pressure region.

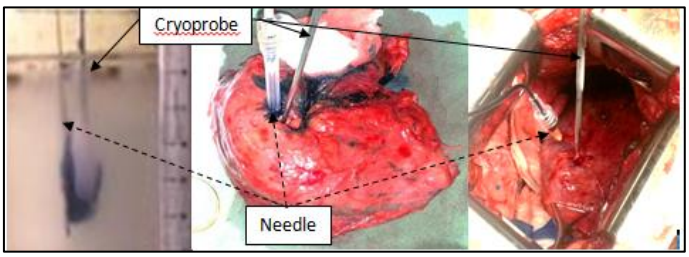

Fig. 3. Examples of freezing-assisted injection procedures. (Left) In vitro simulation in 0.6% agar hydrogel: the 3ml ice zone has an ovoid shape about the cryoprobe and excludes the 1.3ml MB solution that

distributes at the ice-hydrogel interface [37]. There is a 10mm gap between the injection needle and the cryoprobe; (Middle) ex vivo procedure: the needle depth stop sets a 15mm insertion depth and the cryoprobe-needle gap in a freshly resected specimen. (Right) Intraoperative digital photograph of the freezing-and-injection procedure of a peripheral lung tumor conducted on a collapsed lung, before the vascular ligature.

Study groups: In the in vivo group (n=17) - intraoperative freezing and MB injection (n=11) or the MB injection alone (n=6) preceded the vascular dissection and tumor resection. In the ex vivo group (n=16), ten freshly resected tumors were frozen-and-injected to evaluate the MB dye transport and distribution in the non-perfused lung-tumor interface and peritumoral tissue; six tumors were injected ex vivo without simultaneous freezing, as seen in table 2.

Table 2.

Patients Study Groups

SERIES	PROCEDURE		Tumor Volume Vt (cm3)	MB Dose % (Vt)	Ice Zone % (Vt)	Migration Time (min.)
	IN-JECT	FREEZE-INJECT				
In vivo (n=17)	6	11	15.8 (4.1-317)	9 (0.1-46)	19 (1-107)	15 (90)
Ex vivo (n=16)	6	10	17.8 (5.3-84.8)	7 (2-24)	15 (4-57)	15

The median tumor volume Vt, (range) is calculated with the formula: 4/3 pi(r1*r2*r3); the methylene blue (MB) dose and ice zone (IZ) are estimated as a volume percentage of Vt (range). The migration time is the time during which the MB can distribute into the tumor and the lung. In vivo, the grander migration time is due to the tracer transport in the perfused tissue followed by a migration in the non-perfused tissue following the intraoperative vascular ligature-section.*

The intraoperative procedure was as follows: the tumor biopsy was performed far from the injection site, before the injection procedure. On the deflated lung, the needle equipped with its depth stop was inserted in the inner side of the visible and/or palpable edge. The continuous injection of the 1.3ml MB dose took about 2 minutes, an injection rate of about 0.70ml/minute. For the freezing-and-injection procedure, we inserted the cryoprobe tip (Cp) inside the palpable tumor edge; The Cp was always located closer to the tumor center than the needle, as shown in Figure 2. Upon its activation the Cp froze, stuck and helped with keeping the tumor steady during the needle insertion in the tumor inner edge, about 10 to 15 mm apart. We initiated the tracer injection after 30 sec of freeze, and we pursued the freezing during the MB injection for 2 minutes. Next, the active thaw detached t the cryoprobe from the tumor within 2 to 3 seconds. The freeze-injection procedure took about 15 minutes from start to completion. The time available for the evaluation of the tracer distribution into the vascularized tumor and/or the lung parenchyma (Table 2) was about 15 minutes before any lymphovascular dissection, and about 90 minutes before the resection. We recorded the staining dynamics with time-stamped digital photos.

For the ex vivo procedure, at the completion of surgery, we injected sixteen freshly resected samples in the operative room with the prescribed techniques and allowed a 15 minutes migration time for the tracer as seen in table 2. The injection site was not massaged.

Staining evaluation: Following the procedure, the lung-tumor specimen was cross-sectioned in a vertical plane defined by the needle and the probe tracks, and a horizontal plane passing in the middle of the tumor. We measured and took digital photographs of vertical and horizontal cross-sections of the lung-tumor specimen. A macroscopic visual assessment of the staining pattern, localization, and spread, including the previously frozen region was made. The MB dose and the ice zone volume were similar in order to evaluate whether the tumor characteristics and/or their perfusion status would affect the MB distribution pattern. Frozen sections of the blue stained tumor and edge were measured to determine the microscopic distribution of the tracer. The microscopic examination was completed with a conventional formalin fixation and HE staining on all specimen.

Post-operative therapy and follow up: All the patients presenting with stage II to IV disease (n=21) were treated with cisplatin-based doublet adjuvant chemotherapy (ACT), 3 to 4 weeks after the surgery. External beam radiotherapy was associated for one patient. Eleven patients had no adjuvant therapy.

Statistics

Given the limited number of cases and the qualitative aspect of the study, we did not conduct any statistical evaluation.

Conflict of interests

There is no conflict of interests.

3 RESULTS AND DISCUSSION

The staining rate, localization and pattern of methylene blue (MB) within the edge interface, the tumor and the lung exhibited large variations.

Staining rate and spread: The MB constantly stained the lung-tumor interface and migrated within tumor and the surrounding lung. At gross examination of the tumor cross sections the dye was spreading over 30% to 50% of the tumor perimeter for 27/33 (81%) cases, and over 50% of the perimeter for the rest. The stained area was grander, >50%, in the tumor core or in the contiguous lung, respectively for 7/33 (21%) and 6/33 (18%) procedures. This intra- and extra-tumoral localization of the MB tracer was similar for the in vivo and ex vivo cases, regardless of the MB migration time; a time that was inevitably longer in vivo compared to ex vivo as shown in Table 2. In all cases, the MB stained the cryoprobe site either during the thaw of after the full melting of the frozen tissue, but never during the freezing.

Staining pattern: the gross staining pattern was heterogeneous, patchy and mosaic-like, or confluent in the tumor; strikingly, it was homogeneous in the tumor edge and the contiguous lung, as exemplified in table 4 and figure 4. We observed an equivalent pattern in all specimens, regardless of the injection technique -freeze assisted or not- , the tumor pathology, dimension, or perfusion status.

Table **3.**

Lung-tumor interface MB staining.

Tumor + Edge + Lung	ADC	SCC	Large Cell C	Met	Ca.S	Small Cell C	C.oid	**Total**
L + M + S	3	1	2	---	1	---	---	7
M + M + M	10	4	2	2	---	1	1	20
S + L + L	4	2	---	---	---	---	---	6
Total	17	7	4	2	1	1	1	33

On fresh tumor gross sections at visual examination, the MB distributes more largely within edge and tumor in 7 cases (upper row) and within edge and contiguous lung in 6 cases (lower row). In all cases, the tumor edge staining is constant and bidirectional: towards the tumor core and towards the lung, regardless of the tumor characteristics, the blood perfusion status, or the simultaneous freeze. We grade the stain spread on the tumor cross sections (left column) as large (L: >50%), medium (M: 30% to 50%), or small (S: <30%). In 20 cases, the M+M+M category, the stain distributed equally in the tumor, the edge and the lung. ADC: adenocarcinoma; SCC: squamous cell carcinoma; Ca.S: carcinosarcoma; C.oid: carcinoid.

The tracer distributed within the tumor active and necrotic zone (s), within the thawed zone and into the lung parenchyma.

The ice zone (IZ) surrounding the cryoprobe, was purposely of small size, about 15% to 19% of the tumor volume as seen in table 2; we calculated it to be 40% to 50% of the torus equivalent invasion edge model, for the ex

vivo or in vivo procedures (data not shown). Although the IZ was impervious to the simultaneously injected tracer, it did not prevent the dye from migrating towards the tumor core and away from it towards the lung in an injection only-like pattern.

Table 4.

Lung-tumor interface MB staining.

Pat-tern	ADC	SCC	Large Cell C	Met	Ca. S	Small Cell C	C.oid	Total
Con-fluent	11	4	2	1	---	1	1	20
Patchy	6	3	2	1	1	---	---	13
Total	17	7	4	2	1	1	1	33

The tumor-staining pattern is independent of the injection procedure (freezing-assisted or not), tumor characteristics and/or blood perfusion status. ADC: adenocarcinoma; SCC: squamous cell carcinoma; Ca.S: carcinosarcoma; C.oid: carcinoid.

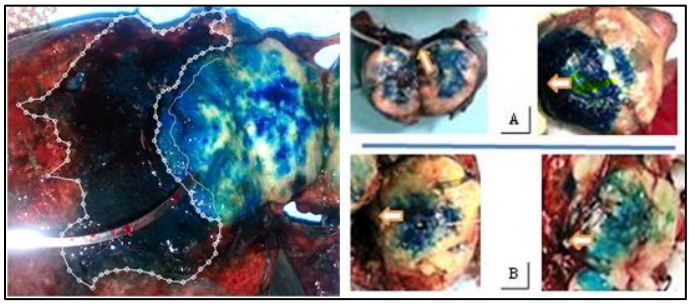

Fig. 4. Staining localization and pattern observed in lobectomy specimens post injection or post freeze-injection. Left: freehand ROI delineation of the homogeneous inner and outer edge staining compared to the patchy staining, >50%, of an ADC tumor core. Right: the homogeneous and constant staining of the invasion edge (arrows) and of the contiguous lung departs from the tumor core patterns: mosaic-like in A, confluent in B. The Mb distributes on both sides of the invasion edge. ADC: adenocarcinoma.

Microscopy: The microscopic examination showed similar in vivo and ex vivo aspects: the dye distributed in the tumor edge matrix, interstitial fluid spaces and randomly within the cells and nuclei. The tumor structures, including the freezing zone, remained recognizable. The necrotic zones and post-freeze alterations were unremarkable as illustrated in Figure 5.

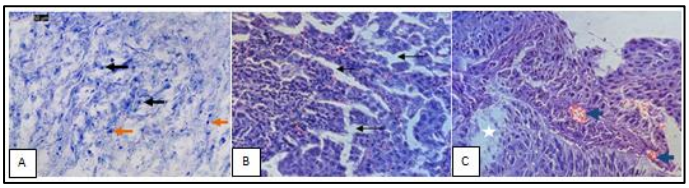

Fig. 5. A: the frozen section (Scale Bar-100µm) of an ADC injected ex vivo evidences a uniform tracer distribution in the stroma, and the random staining of the tumor cells (black arrows) and nuclei (orange arrows). B: an H&E stained ADC section (200X) previously frozen and injected, evidences a predominant papillary structure and an identifiable grading (G3); large intercellular spaces (black arrows) due to post-freeze interstitial edema are also visible. C: an H&E stained SCC section (200X) shows necrotic zones (white star), and early thrombosis of vessel lumens (blue arrows).

Staining dynamics: The tumor and the lung staining was fast and visible within 10 minutes of the injection; however the tracer was not detected in the interlobar, hilar or mediastinal region and lymph nodes at the time of resection, 90 minutes after the injection.

Injection associated devices: The needle depth stop facilitated the injection procedure. In the beginning of our study, we found out that the tumor contours and the edge were not always easy to delineate or palpate; an additional difficulty was to insert a bare needle in the tumor edge while insuring that it did not transfixed the tumor. The self-made depth stop of figure 1 helped with setting an insertion depth and maintaining the needle still during the injection. We also used the sticking effect of the activated cryoprobe to manipulate the tumor and ease the needle insertion during the freezing injection procedure. There was no significant bleeding during or after the removal of the Cp from its tract.

The injection procedure(s) blended well with the normal surgical workflow: The inclusion of the freeze-injection procedure added an average 17 minutes (range, 15-20) to the operative time; it went uneventfully on the 17 in vivo patients. There was no significant loss of MB dose from reflux or leakage. In 6/33 cases a reflux estimated at <100ul for, i.e. 6% of the MB dose, occurred

during the needle removal, and the lost dose was not compensated for. In one case, a minor leakage of the dye occurred in the bronchial tree during a wedge resection. The procedure was not associated with any side effects or intraoperative or postoperative adverse event.

DISCUSSION

Our study primary objective was to investigate the intraoperative distribution pattern of a blue dye tracer injected in the inner side of resectable primary or secondary lung tumors stage I to IV. We selected MB dye as a surrogate for a cytotoxic agent. The ability of a concomitant focal freezing to drive the directional flow of the tracer was explored, and the influence of the blood perfusion status on the dye migration was compared. A secondary objective was to evaluate how well the procedure integrated with the conduct of a conventional surgery. The ultimate objective of our research is to use the knowledge gained from this study for the development of intraoperative, antimetastatic edge-targeting injection techniques during the surgery of lung tumors.

Our results, illustrated in table 3-4 and figure 4, show that the dye distributed constantly and homogeneously within the edge and the contiguous lung; this migration reached also the tumor core where the staining pattern was heterogenous. The tracer localization rate, spread and distribution pattern was unrelated to the injection technique, the volume, pathological characteristics, or the vascular perfusion status of the tumor. The ice zone, conversely to the post-thaw zone, excluded the tracer. In all cases, the dye stained the interstitium of the lung-tumor interface.

The homogeneous staining pattern of the IE, contrasting with the heterogenous tumor staining was striking but predictable. Indeed, when selecting the inner side of the IE for the injection we assumed equivalent fluid transport properties in the edge interstitial fluid space, a space estimated to stretch over the innermost and outermost side of the tumor gross edge [27, 28]. We also hypothesized higher odds of reaching the fluid dissemination pathways with injecting the inner side rather than the outer side of the edge, where watershed regions [32] might have pooled the injected fluid. Given the known properties of the edge interstitium, including similar low interstitial fluid pressure (IFP), interstitial fluid flow (IFF), pore structure and hydraulic conductivity [27], we inferred that the small hydrophilic MB tracer would disperse homogeneously and convectively from the inner edge injection site outwards [33, 34]. Remarkably, a study by Vignaud et al. [26] demonstrated similar homogenous dye distribution pattern at the edge-lung interface, along with a heterogeneous tumor staining. The authors injected trans-bronchially a single low dose of MB, 0.75ml, into lung tumors a few minutes before surgical resection. Although they were targeting the tumor core, their injection-and-pull technique likely reached the tumor inner and outer margin instead. The tumor staining, 29%, was quite large for the injected dose; a fact probably due to the slow injection rate, 0.37ml/min, known for improving the distribution volume [33]. The two-dimensional dye spread observed in our study, although not quantifiable, looks similar; we infer that the needling technique and the site of injection contributed the tracer distribution more than the dose or the injection rate, that was twofold higher compared to Vignaud [26].

The heterogeneous staining pattern of the tumor core, illustrated in figure 4, is not new [24], confirming the heterogeneous structure of most solid tumors. Such heterogeneity complicates the proper delivery of intralesional chemo-gene- or immuno- therapies, which require that these agents reach all tumor cells within the target [14, 19]. Only multiple local injection sites and/or repeated treatment sessions fulfill in part this objective [13, 35], increasing health care costs and constraints for the patients. The bidirectional tracer migration from a single site of injection was unexpected in light of the published techniques of lung tumor chemoablation [13, 14, and 35] that require both intra- and extra-tumoral injections. To the best of our knowledge, it is the first time that the direct injection of MB in the innermost edge of a lung tumor spreads the tracer in this edge and from there in the tumor and in the lung, as illustrated in figure 2. We think that the

injection pressure and resulting pressure gradient created in the edge is the main driver of the drug flow. For Zhang [36] such flow commences at a 24mmHg infusion pressure threshold; over this threshold, the tumor interstitial fluid channels, usually poorly connected, would open and interconnect. We infer that the convergent flow of the tracer towards the tumor core is due to an injection pressure grander than the interstitial fluid pressure. In vivo the IFP is about 25mmHg in the tumor core, and is slightly positive or close to zero mmHg in the edge [12]; ex vivo, in an integral tumor specimen [33] the IFP is also low, ~3mmHg. The higher migration rate of the dye outwards in the lung, although not quantified, would have a similar ground. The low IFP in the edge-lung region would promote a higher migration spread of the dye, a trend seen in Table 3, due to a larger fluid pressure gradient in this region.

The similar staining pattern and migration, observed in vivo and ex vivo, points to the well-known rapid transport of the small tracer into the interstitium [18]; its clearance through the aerogenous and lymphovascular drainage pathways, probably combines equally with the blood capillary clearance, and may explain the absence of specific accumulation in the nodes. The small dose of tracer or the single site of injection [17] may have been additional accumulation-limiting factors. Nevertheless, the presence of the dye within the interstitial fluids warrants its uptake and migration within the lymphovascular network [29].

The successful but unmodified interstitial transport of the dye during the simultaneous focal freezing and injection of the tumor edge was predictable. No injection failure due to needle freezing and fluid crystallization was observed, a confirmation that we had met with the spatial and temporal parameters for a proper freezing-assisted fluid delivery, as previously demonstrated [24, 25] and illustrated in figure 3. The ice zone, although impervious to the co-injected fluid, as expected [24, 37], could not prevent the dye from migrating around the ice margin. The IZ size was likely too small, about 17% of the tumor volume (Table2), to affect the interstitial fluid pressure gradients and the resulting general direction of the flow.

The tumor edge delineation and the needle insertion were two crucial steps of the procedure. The gross margin was the beacon for the needle insertion, but sometimes it was not directly visible or palpable. The use of atraumatic Duval clamps helped with presenting the tumor edge to the needle; as did the cryoprobe, which could stuck to, lift and orientate the tumor, as described by others [38, 39].

Overall, we estimated the spatial positioning of the needle to be within ± 3mm. In seven in vivo cases, the lung was injected due to an unwanted needle motion off target, and we had to reposition the needle; a fact that lead us to make a depth stop for that small needle diameter. Intraoperative ultrasound for the determination of the tumor edge and more precise needle guidance was not used, due to the likely prolongation of anesthesia and known limitations of ultrasound imaging in the lung [16]. Despite our rough estimate of the exact needle tip location, the consistent patterns of edge staining observed in our study may indicate that the whole edge fluid space is a proper target for an interstitial injection. However, the width of this interstitial fluid space is an estimate [28, 40], and we could not assess a posteriori the exact location of the needle tip due to the rapid spread of the dye.

MB was selected as a surrogate for a chemotherapeutic agent that we could inject in similar conditions. MB is a weak basic drug that gets protonated in the acidic environment of the tumor edge [41] and therefore may disperse mostly in the interstitial fluid space of the edge, as it seems from our study. We anticipate that the chemotherapeutics doxorubicin, mitoxantrone, vincristine, and vinblastine, which are also protonated in acidic environment, and display a decreased cellular uptake [42], would behave like the MB [43]. Additionally the MB tracer could serve as a co-marker of the distribution pattern for the above drugs, except mitoxantrone, a known chromophore. We successfully demonstrated in an animal tumor model the freezing-assisted injection and distribution of MB combined with epirubicin, another weak basic cytotoxic, at the tumor edge; the cell kill was predominant at this stained area [24].

Both injection procedures integrated well within the conduct of conventional surgery at open thoracotomy

approach. Even though the freezing-assisted injection procedure took longer than the single injection, its duration was in the range of published results for intraoperative lymphatic mapping [18]. Overall, the absence of procedural complications, even in the rare occurrence of dye leakage in the bronchial tree, one in our study confirms the safety of the technique [14, 19, 35].

We are aware of some limitations of the study, such as the small number of patients, and the qualitative evaluation due to the heterogeneity of the sampled tumors; both prohibited any statistical analysis. We evaluated the MB distribution pattern by direct visualization at the macroscopic level on a limited number of tumor sections, thus making impossible a precise distribution volume estimate. A specific preparation of the fixated, paraffin-embedded sample [26] might have brought additional microscopic details, compared to those reported only on frozen sections.

Overall, we think this simple study has important clinical implications. The first of which relates to the relative imprecision of the peritumoral techniques of injection, such as used for lymphatic mapping or chemoablation. In light of these preliminary results, any objective analysis of an intraoperative injection made at the tumor edge, either for diagnostic or therapeutic purpose, should use a readily locatable site marker evidencing the needle location; the mere description of this location looks insufficient to analyze a possible injection site and distribution related effect. The second implication relates to the likely but unknown rate and spread of edge staining during conventional peritumoral, multi-quadrant injection for intraoperative lymphatic mapping. A prospective clinical study using blue dye tracer(s) should be conducted; which might bring valuable information on the drug transport in the edge fluid space, and the tumor; further contributing to the development of novel intraoperative antimetastatic edge-targeting therapeutic injection techniques. Such targeting with cytotoxic drug(s) could be the initial rather than the final step of the chemoablative methods currently in use. The outer edge is already the target of no-touch thermal or non-thermal tumor ablation techniques that aim at decreasing the intraoperative cell dissemination [44]. The third implication is a procedural confirmation that the ice margin must cover the whole tumor edge to prevent the co-injected dye from permeating the frozen tumor. However, the post thaw region behaves as a trap for the dye, and therefore a possible modulator of the drug pharmacokinetics during resection [24].

CONCLUSIONS

The inner side of the invasion edge of resectable primary or secondary lung tumors looks a suitable location for directly injecting and distributing the methylene blue tracer within the interstitium and fluid-draining pathways of the lung tumor interface. The edge interstitial fluid space pools and disperses the MB dye bi-directionally within the tumor and the lung, regardless of injection technique, tumor characteristics or blood perfusion status. Fresh resection specimens are convenient tools to investigate further the edge injection parameters, and optimize the drug transport effectiveness to the interstitial fluid pathways of cell dissemination during surgery.

LIST OF ABBREVIATIONS

IT: Intra tumor; PT: peritumoral; IZ: Ice zone; MB: Methylene blue; Cp: cryoprobe; FAI: Freeze-assisted injection

DECLARATIONS

The Study received clearance from the Ethics Committee of the Department of Thoracic Surgery, Wroclaw Medical University, Wybrzeże L. Pasteura 1, 50-367 Wrocław, Poland, NIP 896-000-57-79.

All the patients provided their informed consent before the procedure.

All data generated or analyzed during this study are included in this published article

FUNDING

The Study was conducted under a grant # ST 790 from: Wroclaw Medical University, ul. Grabiszyńska, 105 53-439 Wroclaw, Poland. Tel. 71 33 49 400 or 71 334 94 75; Fax. 71 334 96 03; E-mail: barbara.mroz@umed.wroc.pl or adam.rzechonek@umed.wroc.pl

AUTHORS' CONTRIBUTIONS

AR contributed to the study design, the surgical data

collection, data analysis, and manuscript revision; conducted the surgical procedures. PB and MM contributed equally to the study data collection and analysis. BMB, JA and LF contributed equally to the pathological data collection and analysis. WB contributed to the study coordination, data analysis, and manuscript revision. PLP conceived the study and the delivery technique, contributed to the study design and coordination, data analysis, and writing the manuscript. All authors read and approved the final manuscript.

REFERENCES

1 Kelsey, C. R., Marks, L. B., Hollis, D., Hubbs, J. L., Ready, N. E., D'Amico, T. A., & Boyd, J. A. (2009). Local recurrence after surgery for early stage lung cancer: An 11-year experience with 975 patients. Cancer, 115(22), 5218–5227. http://doi.org/10.1002/cncr.24625

2 Matsangou, M., Santos, E. S., Raez, L. E., Gomez, J. E., Dinh, V., & Savaraj, N. (2014). Early-stage non-small-cell lung cancer: Overview of adjuvant chemotherapy and promising advances. Lung Cancer Management, 3(1), 85–99.

3 Coffey, J. C., Wang, J. H., Smith, M. J. F., Bouchier-Hayes, D., Cotter, T. G., & Redmond, H. P. (2003). Excisional surgery for cancer cure: Therapy at a cost. Lancet Oncology, 4(12), 760–768. http://doi.org/10.1016/S1470-2045(03)01282-8

4 Polzer, B., & Klein, C. A. (2013). Metastasis Awakening: The challenges of targeting minimal residual cancer. Nature Medicine, 19(3), 274–275. http://doi.org/10.1038/nm.3121

5 Ceelen, W., Pattyn, P., & Mareel, M. (2014). Surgery, wound healing, and metastasis: Recent insights and clinical implications. Critical Reviews in Oncology/Hematology. http://doi.org/10.1016/j.critrevonc.2013.07.008

6 Ceelen, W. P., Morris, S., Paraskeva, P., & Pattyn, P. (2007). Surgical trauma, minimal residual disease and locoregional cancer recurrence. Cancer Treatment and Research, 134, 51–69. Retrieved from http://www.ncbi.nlm.nih.gov/pubmed/17633047

7 Baba, T., Uramoto, H., Kuwata, T., Takenaka, M., Chikaishi, Y., Oka, S., … Tanaka, F. (2013). Intrapleural chemotherapy improves the survival of non-small cell lung cancer patients with positive pleural lavage cytology. Surgery Today, 43(6), 648–653. http://doi.org/10.1007/s00595-012-0281-y

8 Liang, Y., & Wakelee, H. A. (2013). Adjuvant chemotherapy of completely resected early stage non-small cell lung cancer (NSCLC). Translational Lung Cancer Research, 2(5), 403–410. http://doi.org/10.3978/j.issn.2218-6751.2013.07.01

9 Sawabata, N., Kitamura, T., Nitta, Y., Taketa, T., Ohno, T., Fukumori, T., … Nakamura, T. (2017). Lung cancer biopsy dislodges tumor cells into circulating blood. Journal of Cancer Metastasis and Treatment, 3(1), 16. http://doi.org/10.20517/2394-4722.2016.67

10 Gaikwad, A., Souza, C. A., Inacio, J. R., Gupta, A., Sekhon, H. S., Seely, J. M., … Gomes, M. M. (2014). Aerogenous metastases: a potential game changer in the diagnosis and management of primary lung adenocarcinoma. American Journal of Roentgenology, 203(6), W570–W582. http://doi.org/10.2214/AJR.13.12088

11 Pandya, P., Orgaz, J. L., & Sanz-Moreno, V. (2016). Modes of invasion during tumour dissemination. Molecular Oncology, 11, 1–23. http://doi.org/10.1002/1878-0261.12019

12 Wiig, H., Tenstad, O., Iversen, P., Kalluri, R., Bjerkvig, R., Freitas, I., … Haggerty, A. (2010). Interstitial fluid: the overlooked component of the tumor microenvironment? Fibrogenesis & Tissue Repair, 3(1), 12. http://doi.org/10.1186/1755-1536-3-12

13 Celikoglu, F., Celikoglu, S. I., & Goldberg, E. P. (2010). Intratumoural chemotherapy of lung cancer for diagnosis and treatment of draining lymph node

metastasis. Journal of Pharmacy and Pharmacology, 62(3), 287–293. http://doi.org/10.1211/jpp/62.03.0001

14

15 Mehta, H. J., Begnaud, A., Penley, A. M., Wynne, J., Malhotra, P., Fernandez-Bussy, S., … Jantz, M. A. (2015). Restoration of Patency to Central Airways Occluded by Malignant Endobronchial Tumors Using Intratumoral Injection of Cisplatin. Annals of the American Thoracic Society, 12(9), 1345–50. http://doi.org/10.1513/AnnalsATS.201503-131OC

16

17 Goldberg, E. P., Hadba, A. R., Almond, B. a, & Marotta, J. S. (2002). Intratumoral cancer chemotherapy and immunotherapy: opportunities for nonsystemic preoperative drug delivery. The Journal of Pharmacy and Pharmacology, 54(2), 159–180. http://doi.org/10.1211/0022357021778268

18

19 Tempany, C. M. C., Jayender, J., Kapur, T., Bueno, R., Golby, A., Agar, N., & Jolesz, F. A. (2015). Multimodal imaging for improved diagnosis and treatment of cancers. Cancer, 121(6), 817–27. http://doi.org/10.1002/cncr.29012

20 Hachey, K. J., & Colson, Y. L. (2014). Current Innovations in Sentinel Lymph Node Mapping for the Staging and Treatment of Resectable Lung Cancer. Seminars in Thoracic and Cardiovascular Surgery, 26(3), 201–209. http://doi.org/10.1053/j.semtcvs.2014.09.001

21 Meyer, A., Cheng, C., Antonescu, C., Pezzetta, E., Bischof-Delaloye, A., & Ris, H.-B. (2007). Successful migration of three tracers without identification of sentinel nodes during intraoperative lymphatic mapping for non-small cell lung cancer. Interactive Cardiovascular and Thoracic Surgery, 6(2), 214–8. http://doi.org/10.1510/icvts.2006.141911

22 Mehta, H. J., Begnaud, A., Penley, A. M., Wynne, J., Malhotra, P., Fernandez-Bussy, S., … Jantz, M. A. (2015). Treatment of isolated mediastinal and hilar recurrence of lung cancer with bronchoscopic endobronchial ultrasound guided intratumoral injection of chemotherapy with cisplatin. Lung Cancer, 90(3), 542–547. http://doi.org/10.1016/j.lungcan.2015.10.009

23 Stylianopoulos, T., Martin, J. D., Snuderl, M., Mpekris, F., Jain, S. R., & Jain, R. K. (2013). Co-evolution of solid stress and interstitial fluid pressure in tumors during progression: Implications for vascular collapse. Cancer Research, 73(13), 3833–3841. http://doi.org/10.1158/0008-5472.CAN-12-4521

24 Shentu, Y., Zhang, L., Gu, H., Mao, F., Cai, M., Ding, Z., & Wang, Z. (2014). A new technique combining virtual simulation and methylene blue staining for the localization of small peripheral pulmonary lesions. BMC Cancer, 14, 79. http://doi.org/10.1186/1471-2407-14-79

25 Lim, E. J., Oak, C. H., Heo, J., & Kim, Y. H. (2013). Methylene blue-mediated photodynamic therapy enhances apoptosis in lung cancer cells. Oncology Reports, 30(2), 856–862. http://doi.org/10.3892/or.2013.2494

26 Shafiei, S., Bagheri, R., Sadri, K., Jafarian, A. H., Attaran, D., Lari, S. M., & Basiri, R. (2015). Sentinel node mapping for intra-thoracic malignancies: systematic review of the best available evidence, 2(2), 52–57. Retrieved from http://rcm.mums.ac.ir/article_3865_556.html

27 He, X., Xiao, Y., Zhang, X., Du, P., Zhang, X., Li, J., … Le Pivert, P. (2016). Percutaneous Tumor Ablation: Cryoablation Facilitates Targeting of Free Epirubicin-Ethanol-Ioversol Solution Interstitially Co-injected in a Rabbit VX2 Tumor Model. Technology in Cancer Research & Treatment, 15(4), 597–608. http://doi.org/10.1177/1533034615593855

28 Le Pivert, P. J., Morrison, D. R., Haddad, R. S., Renard, M., Aller, A., Titus, K., & Doulat, J. (2009). Percutaneous tumor ablation: microencapsulated

echo-guided interstitial chemotherapy combined with cryosurgery increases necrosis in prostate cancer. Technology in Cancer Research & Treatment, 8(3), 207–216. Retrieved from http://www.ncbi.nlm.nih.gov/pubmed/19445538

29 Vignaud, J.-M., Ménard, O., Weinbreck, N., Siat, J., Borrelly, J., Marie, B., … Martinet, Y. (2006). Evaluation of the spatial diffusion of methylene blue injected in vivo by bronchoscopy into non-small cell lung carcinoma. Respiration; International Review of Thoracic Diseases, 73(5), 658–63. http://doi.org/10.1159/000094392

30 Boucher, Y., Baxter, L. T., & Jain, R. K. (1990). Interstitial Pressure Gradients in Tissue-isolated and Subcutaneous Tumors: Implications for Therapy. Cancer Research, 50(15), 4478–4484. Retrieved from http://cancerres.aacrjournals.org/content/50/15/4478

31 Giraud, P., Antoine, M., Larrouy, A., Milleron, B., Callard, P., De Rycke, Y., … Touboul, E. (2000). Evaluation of microscopic tumor extension in non-small-cell lung cancer for three-dimensional conformal radiotherapy planning. International Journal of Radiation Oncology, Biology, Physics, 48(4), 1015–24. Retrieved from http://www.ncbi.nlm.nih.gov/pubmed/11072158

32 Munson, J. M., & Shieh, A. C. (2014). Interstitial fluid flow in cancer: implications for disease progression and treatment. Cancer Management and Research, 6, 317–328. http://doi.org/10.2147/CMAR.S65444

33 Soltani, M., Chen, P., Babich, J., Kierstead, D., & Graham, W. (2011). Numerical Modeling of Fluid Flow in Solid Tumors. PLoS ONE, 6(6), e20344. http://doi.org/10.1371/journal.pone.0020344

34 Polacheck, W. J., Charest, J. L., & Kamm, R. D. (2011). Interstitial flow influences direction of tumor cell migration through competing mechanisms. Proceedings of the National Academy of Sciences of the United States of America, 108(27), 11115–20. http://doi.org/10.1073/pnas.1103581108

35 Estourgie, S. H., Nieweg, O. E., Valdés Olmos, R. A., Th Rutgers, E. J., & Kroon, B. B. R. (2003). Intratumoral versus intraparenchymal injection technique for lymphoscintigraphy in breast cancer. Clinical Nuclear Medicine, 28(5), 371–374. http://doi.org/10.1097/01.RLU.0000063409.68758.D4

36 McGuire, S., & Yuan, F. (2001). Quantitative analysis of intratumoral infusion of color molecules. American Journal of Physiology - Heart and Circulatory Physiology, 281(2), H715–H721. Retrieved from http://ajpheart.physiology.org/content/281/2/H715

37 Jain, R. K., Martin, J. D., & Stylianopoulos, T. (2014). The role of mechanical forces in tumor growth and therapy. Annual Review of Biomedical Engineering, 16, 321–346. http://doi.org/10.1146/annurev-bioeng-071813-105259

38 Hohenforst-Schmidt, W., Zarogoulidis, P., Darwiche, K., Vogl, T., Goldberg, E. P., Huang, H., … Brachmann, J. (2013). Intratumoral chemotherapy for lung cancer: re-challenge current targeted therapies. Drug Design, Development and Therapy, 7, 571–83. http://doi.org/10.2147/DDDT.S4639336-

39 Zhang, X.Y., Luck, J., Dewhirst, M. W., & Yuan, F. (2000). Interstitial hydraulic conductivity in a fibrosarcoma. American Journal of Physiology - Heart and Circulatory Physiology, 279(6).

40 Le Pivert, P. J. (2017) Translational Cryosurgery in Lung Tumor Therapy, Cryoimmunology, Cryochemotherapy, Nanocryosurgery: basics and applications. In H. Wang, K. Xu, P. Littrup, (Eds.) Cryosurgery for Lung Cancer (to be published). Wien, New York: Springer. Retrieved from https://www.researchgate.net/publication/305620390

41 Maiwand, M. O., & Asimakopoulos, G. (2004). Cryosurgery for lung cancer: clinical results and technical aspects. Technology in Cancer Research & Treatment, 3(2), 143–50. Retrieved from http://www.ncbi.nlm.nih.gov/pubmed/15059020

42 Polk, W., Fong, Y., Karpeh, M., & Blumgart, L. H. (1995). A technique for the use of cryosurgery to assist hepatic resection. Journal of the American College of Surgeons, 180(2), 171–176.

43 Hassid, Y., Furman-Haran, E., Margalit, R., Eilam, R., & Degani, H. (2006). Noninvasive magnetic resonance imaging of transport and interstitial fluid pressure in ectopic human lung tumors. Cancer Research, 66(8), 4159–4166. http://doi.org/10.1158/0008-5472.CAN-05-3289

44 Gatenby, R. A., Gawlinski, E. T., Gmitro, A. F., Kaylor, B., & Gillies, R. J. (2006). Acid-mediated tumor invasion: A multidisciplinary study. Cancer Research, 66(10), 5216–5223. http://doi.org/10.1158/0008-5472.CAN-05-4193

45 Trédan, O., Galmarini, C. M., Patel, K., & Tannock, I. F. (2007). Drug resistance and the solid tumor microenvironment. Journal of the National Cancer Institute, 99(19), 1441–1454. http://doi.org/10.1093/jnci/djm135

46 Raghunand, N., & Gillies, R. J. (2000). pH and drug resistance in tumors. Drug Resistance Updates : Reviews and Commentaries in Antimicrobial and Anticancer Chemotherapy, 3(1), 39–47. http://doi.org/10.1054/drup.2000.0119

47 Morimoto, N., Isoda, N., Takaoka, Y., Hirosawa, T., Watanabe, S., Otake, T., … Yamamoto, H. (2017). Short-Term Results of Laparoscopic Radiofrequency Ablation Using a Multipolar System for Localized Hepatocellular Carcinoma. Liver Cancer, 6(2), 137–145. http://doi.org/10.1159/000450925

Received: 13-Jun. – 2017
Accepted: 21-Sep. - 2017